Spectroscopic factors in the N=20 island of inversion: The Nilsson strong-coupling limit

A. O. Macchiavelli, H. L. Crawford, C. M. Campbell, R. M. Clark, M. Cromaz, P. Fallon, M. D. Jones, I. Y. Lee, A. L. Richard, and M. Salathe

Phys. Rev. C **96**, 054302 — Published 2 November 2017

DOI: 10.1103/PhysRevC.96.054302

Spectroscopic Factors in the $N = 20$ Island of Inversion: The Nilsson Strong Coupling Limit

A. O. Macchiavelli[1], H. L. Crawford[1], C. M. Campbell[1], R. M. Clark[1],
M. Cromaz[1], P. Fallon[1], M. D. Jones[1], I. Y. Lee[1], A. L. Richard[2], and M. Salathe[1]
[1]*Nuclear Science Division, Lawrence Berkeley National Laboratory, Berkeley, CA 94720, USA and*
[2]*Department of Physics and Astronomy, Ohio University, Athens, OH 45701, USA*

Spectroscopic factors, extracted from one-neutron knockout and Coulomb dissociation reactions, for transitions from the ground state of ^{33}Mg to the ground-state rotational band in ^{32}Mg, and from ^{32}Mg to low-lying negative parity states in ^{31}Mg, are interpreted within the rotational model. Associating the ground state of ^{33}Mg and the negative parity states in ^{31}Mg with the $\frac{3}{2}[321]$ Nilsson level, the strong coupling limit gives simple expressions that relate the amplitudes ($C_{j\ell}$) of this wavefunction with the measured cross-sections and derived spectroscopic factors ($S_{j\ell}$). To obtain a consistent agreement with the data within this framework, we find that one requires a modified $\frac{3}{2}[321]$ wavefunction with an increased contribution from the spherical $2p_{3/2}$ orbit as compared to a standard Nilsson calculation. This is consistent with the findings of large scale Shell Model calculations and can be traced to weak binding effects that lower the energy of low-ℓ orbitals.

PACS numbers: 21.10.Jx, 25.55.Hp, 27.30.+t

I. INTRODUCTION

Understanding the so-called "Islands of Inversion" has been the subject of intense work, both experimentally and theoretically [1–3]. As a clear manifestation of the universal phenomenon of shape-coexistence, found in several regions of the nuclear chart, its driving mechanism is now rather well understood. The "inversion" found in neutron-rich nuclei with $N = 8$, 20, and 40 originates from the removal of protons from the corresponding spherical doubly-magic nuclei, $^{16}O_8$, $^{40}Ca_{20}$, and $^{68}Ni_{40}$, which induces changes in the effective single-particle energies (ESPEs), largely due to the monopole average of the central and spin-isospin components of the nuclear force [4]. The delicate balance between the monopole effects, the residual pairing, and quadrupole interactions leads to a competition between spherical and deformed configurations. At some point, the quadrupole correlations dominate over pairing and erode the shell gaps, leading to deformed ground states in nuclei expected, *a-priori*, to be semi-magic and spherical.

Perhaps the best known example is at $N = 20$, where the nucleus ^{32}Mg takes center stage. Deformed intruder configurations, with neutron pairs promoted from the sd to the fp shell across the narrowed N=20 gap, are energetically favored [5–8], leading to a well-developed deformation in the ground states of the affected nuclei.

The use of knock-out reactions (KO), combined with structure input from state-of-the-art Shell Model calculations has proven a powerful tool to elucidate the mechanism discussed above [9]. However, based on the fact that nuclei inside the islands are well deformed, it is of interest to consider the description of these reactions in a rotational framework. Indeed, the single-particle levels at $N = 20$ give rise to underlying symmetries – quasi-SU(3) for neutrons in the pf-shell, pseudo-SU(3) for neutron holes in the sd-shell and quasi-SU(3) for protons in the sd-shell [10] – that make a natural connection between the spherical shell model and the deformed mean-field of the Nilsson model [11].

In the odd-A nuclei surrounding ^{32}Mg, energy levels, electromagnetic transitions and magnetic moments [12–16] can be described in leading-order rotational motion within the Nilsson scheme. These observables are sensitive to the intrinsic wave-functions, and it is naturally of interest to map directly the amplitudes of the relevant Nilsson levels. Such mapping will specifically provide unique insight on the underlying deformed mean-field far from stability, where the effects of weak binding are important [17], and are not captured in the modified-harmonic-oscillator (MHO) potential used in standard Nilsson calculations.

We discuss here the description and interpretation of one neutron removal in the Nilsson strong coupling limit, applying the formalism developed for transfer reactions (see Ref. [18] for a review). Within this approach, we view the 1n-removal reactions as a proxy for the (p, d) reaction, and relate measured spectroscopic factors directly to Nilsson wavefunction amplitudes.

II. THE METHOD

Making the well justified assumption of deformed ground states, the Nilsson strong-coupling limit captures the main ingredients to describe nuclei in the N=20 Island of Inversion, and results in simple relations from which the underlying physics emerges naturally, providing a complementary, and perhaps even more intuitive, alternative to the spherical shell model. For an application to the study of deformed states around ^{20}Ne and ^{24}Mg see for example Refs. [19, 20]. Let us consider the case of the $\frac{3}{2}[321]$ level near the neutron Fermi surface at N=20 and of particular relevance to both ^{31,33}Mg. In the $|j, \ell\rangle$ basis, the wavefunction for this Nilsson level is of the form:

$$|\tfrac{3}{2}[321]\rangle = C_{3/2,1}|p_{3/2}\rangle + C_{5/2,3}|f_{5/2}\rangle + C_{7/2,3}|f_{7/2}\rangle \quad (1)$$

where $C_{j,l}$ are the Nilsson wavefunction amplitudes describing the expansion of the deformed wavefunction in the spherical basis.

Following Ref. [18], the 1n-removal cross-section from the initial ground state $|I_i K_i\rangle$ of the target, to a final state $|I_f K_f\rangle$ in the product nucleus, can be written in terms of the Nilsson amplitudes:

$$\begin{aligned} \frac{d\sigma}{d\Omega} &= \sum_{j,\ell} g^2 \langle I_i j K_i \Delta K | I_f K_f\rangle^2 C_{j,\ell}^2 \langle \phi_f|\phi_i\rangle^2 \sigma_\ell^{-1n} \\ &= \sum_{j,\ell} S_{j,\ell} \times \sigma_\ell^{-1n} \end{aligned} \quad (2)$$

where σ_ℓ^{-1n} is the 1n-removal single-particle cross-section for a given orbital angular momentum transfer (ℓ), and $S_{j,\ell}$ is the spectroscopic factor for a given orbital. The factor g^2 is related to the symmetry of the collective wavefunction, $g^2 = 2$ if $I_i = 0$ or $K_f = 0$; otherwise $g^2 = 1$. The core overlap between the initial and final states, $\langle\phi_f|\phi_i\rangle$, is assumed to be unity.

In Fig. 1 we show schematically the situations we will consider in our analysis of ^{33}Mg to ^{32}Mg and ^{32}Mg to ^{31}Mg in the N=20 Island of Inversion. The experimental cross-sections, by way of the spectroscopic factors, together with the normalization condition of the wavefunction, allow us to directly obtain the three $C_{j,\ell}^2$ amplitudes in Eq. 1 at N=21 and N=20.

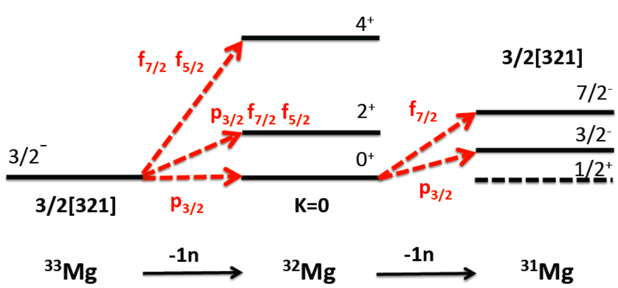

FIG. 1: Schematic representation of the possible transitions for the reactions analyzed in this work. Both $\ell = 1$ and $\ell = 3$ transitions are allowed in both cases considered.

III. RESULTS

A. ^{33}Mg(-1n)^{32}Mg

Ref. [21] reported the results of a neutron-removal experiment performed at the FRS/GSI, where inclusive cross-sections and longitudinal momentum distributions for the reaction ^{33}Mg(-1n)^{32}Mg on a carbon target at 898 MeV/A were measured. More recently, direct experimental evidence of a multiple particle-hole ground state configuration in ^{33}Mg was reported, following an intermediate energy (400 MeV/A) direct Coulomb dissociation measurement, also performed at GSI [22]. Spectroscopic factors, $S_{j,\ell}$, derived from those measurements and reported in Ref. [21], are summarized in Table I.

TABLE I: Experimental spectroscopic factors for ^{33}Mg(-1n)^{32}Mg compared to the calculations using amplitudes obtained with the standard Nilsson parameters and empirically adjusted to the data (see text).

Final State	Energy [MeV]	ℓ	Experimental $S_{j,\ell}$ [21]	[22]	Calculated $S_{j,\ell}$ Nilsson	Empirical
0^+	0.00	1	$0.6^{+0.3}_{-0.5}$	0.19±0.1	0.05	0.24
2^+	0.89	1	$0.5^{+0.7}_{-0.3}$		0.05	0.24
		3	$0.5^{+0.2}_{-0.5}$		0.34	0.18
4^+	2.32	3	–	–	0.55	0.33

For the particular case of a final state with $|I_f, K_f = 0\rangle$, as is the case for ^{33}Mg(-1n)^{32}Mg, the expression for the spectroscopic factors entering Eq. (2) is:

$$S_{j,\ell}(-1n) = 2\langle \frac{3}{2}\ j\ \frac{3}{2}\ \ -\frac{3}{2}|I\ 0\rangle^2 C_{j,\ell}^2$$

As indicated in Fig. 1, the $\ell = 1$ transitions to the 0^+ and 2^+ states depend only on the $p_{3/2}$ amplitude, while the $\ell = 3$ transitions to the 2^+ and 4^+ states involve a sum of the $f_{5/2}$ and $f_{7/2}$ amplitudes. In comparing with the experimental data we consider first a Nilsson calculation with standard input parameters, Ref. [23, 24]. For a deformation of $\epsilon_2 \approx 0.4$, in line with the analysis in Ref. [25], such a standard Nilsson description yields amplitudes: $C_{3/2,1}$ = -0.32, $C_{7/2,3}$ = 0.92, and $C_{5/2,3}$ = -0.22, which fail to reproduce the measured spectroscopic factors (see Table I). In particular, we note the fact that the large amplitude of the $f_{7/2}$ orbit would be consistent with a trend favoring the knockout to the 4^+ member of the ground-state rotational band, clearly not observed in either of the recent experiments.

As discussed earlier, one can reverse the argument and find the Nilsson amplitudes that provide a more consistent description of the experimental results. We make an empirical adjustment to reproduce the weighted mean (0.21 ± 0.1) of the data from [21, 22] for the ground state and determine $C_{3/2,1}^2 = 0.42 \pm 0.2$. However, given the uncertainties in the data, it is not possible to uniquely determine the other amplitudes from the spectroscopic factors. For this, we also require the reproduction of the ground state magnetic moment in ^{33}Mg [16], which can be written in terms of the Nilsson amplitudes in Eq. 1 as:

$$\mu = \frac{3}{5}(g_s\langle s_3\rangle + g_R)$$

$$\langle s_3 \rangle = \frac{1}{2}\Big(C^2_{3/2,1} + \frac{3}{7}(C^2_{7/2,3} - C^2_{5/2,3}) - \frac{4\sqrt{10}}{7} C_{7/2,3}C_{5/2,3}\Big) \quad (3)$$

where g_s and g_R the spin and rotational gyromagnetic factors, and $\langle s_3 \rangle$ the spin projection on the symmetry axis. Following Ref. [15] we use $g_s = -3.83$ and $g_R = 0.3$. After fixing $C_{3/2,1}$ to the value determined above we solve for the values of $C_{7/2,3}$ and $C_{5/2,3}$ that reproduce μ and satisfy the wavefunction normalization condition, as shown in Fig. 2. We consider only positive values of $C_{7/2,3}$, so that the phases follow the signs in the Nilsson calculations [23, 24]. While there are two possible such solutions, it is expected that $|C_{7/2,3}| > |C_{5/2,3}|$. Thus, we choose the one corresponding to $C_{7/2,3} = 0.75$ and obtain the empirical wavefunction†:

$$|\tfrac{3}{2}[321]\rangle = (-0.65 \pm 0.15)|p_{3/2}\rangle + (0.75^{+0.13}_{-0.23})|f_{7/2}\rangle + (-0.12^{+0.08}_{-0.22})|f_{5/2}\rangle$$

and the spectroscopic factors shown in the last column of Table I.

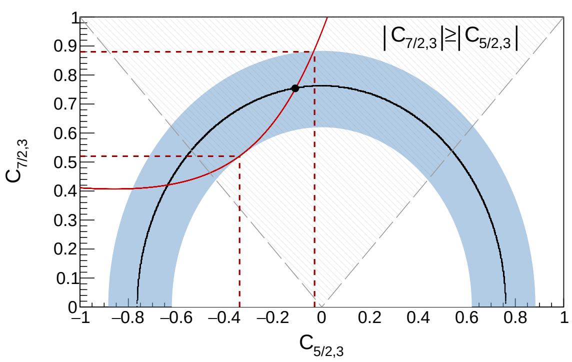

FIG. 2: Two-dimensional plot showing the possible solutions of Eqs. 3 that reproduce the experimental magnetic moment (red line). The intersection with the normalization condition (black line and blue shaded area reflecting the uncertainty in $C_{3/2,1}$) together with the requirement that $|C_{7/2,3}| > |C_{5/2,3}|$ (shaded grey area) determines our adopted solution (solid circle).

This result is in agreement with the conclusions of Refs. [21, 22] where the authors pointed out the increased contribution from the $2p_{3/2}$ orbital required to explain the observations, which is suggestive of its lowering compared to existing model predictions. In fact, the equal amplitudes, $C_{3/2,1} \approx C_{7/2,3}$, needed in our analysis would suggest that the $2p_{3/2}$ and $1f_{7/2}$ spherical orbits get closer in energy, as anticipated in Ref. [17] due to the weak binding effects expected for the $\ell = 1$ orbits.

† The uncertainty is dominated by the error associated with $C^2_{3/2,1}$; the error on the experimental magnetic moment is negligible. Changes to the values of g_s and g_R will, of course, change the empirical values of the other two amplitudes but without affecting the conclusions.

TABLE II: Same as in Table I, experimental spectroscopic factors for ^{32}Mg(-1n)^{31}Mg to negative parity states are compared to the Nilsson predictions.

Final State	Energy [MeV]	ℓ	$S_{j\ell}$ [26]	Calculated $S_{j\ell}$ Nilsson	Empirical
$3/2^-$	0.22	1	$0.59^{+0.11}_{-0.11}$	0.2	0.59
$7/2^-$	0.46	3	$1.24^{+0.4}_{-0.4}$	1.7	1.2

We would like to stress the importance of combining both electromagnetic properties and the spectroscopic factor measurements to determine the single-particle wavefunctions in a consistent analysis. In particular, as several solutions satisfy Eqs. 3, the magnetic moment alone in ^{33}Mg can be explained with the standard Nilsson amplitudes mentioned earlier [15]. However, those amplitudes do not reproduce the results in Table I.

B. ^{32}Mg(-1n)^{31}Mg

The 1n-KO reaction from ^{32}Mg was studied at the NSCL and spectroscopic factors to the low-lying negative parity states in ^{31}Mg were extracted [26]. In this case the final states are assumed to be the two lowest levels of the rotational band built on the Nilsson $\frac{3}{2}[321]$ level discussed above. Because of the angular momentum selection rules imposed by the Clebsch-Gordan coefficients in Eq. 2 the spectroscopic factors in this case directly project out the amplitudes of the wavefunction, ie.

$$S_{3/2,1}(-1n) = 2C^2_{3/2,1}$$

and

$$S_{7/2,3}(-1n) = 2C^2_{7/2,3}$$

In Table II the experimental data are compared with the Nilsson results. As before, a standard Nilsson wavefunction does not provide good agreement with the data. The adjusted amplitudes obtained from the $S_{j,\ell}$, together with the normalization condition give:

$$|\tfrac{3}{2}[321]\rangle \approx (-0.54 \pm 0.05)|p_{3/2}\rangle + (0.79 \pm 0.13)|f_{7/2}\rangle + (-0.29 \pm 0.36)|f_{5/2}\rangle$$

Given the uncertainties in the derived amplitudes, this is consistent with the wavefunction obtained earlier, requiring the increase of the $2p_{3/2}$ component relative to those of the f orbits.

IV. CONCLUSION

Guided by the formalism developed for studies of single-nucleon transfer reactions in deformed nuclei, we have analyzed recent experimental data on 1n-removal reactions from ^{33}Mg and ^{32}Mg in the rotational strong-coupling limit. While a standard $\frac{3}{2}[321]$ Nilsson level wavefunction does not reproduce the measured spectroscopic factors, modified amplitudes, with a relative increase of the $2p_{3/2}$ component, provide a reasonable description of the data. The empirically adjusted wavefunctions can be understood by a reduction of the N=28, $1f_{7/2} - 2p_{3/2}$, gap in the standard Nilsson MHO potential by ~ 3 MeV, consistent with the trend of the ESPEs used in Shell-Model calculations and the more realistic spherical orbits that originate from a Wood-Saxon type potential.

Based on the fact that intruder deformed configurations dominate the low-lying structure of nuclei within the Islands of Inversion, the Nilsson formalism provides an intuitive and simple approach to obtain important structure information from direct reactions. As shown in this work and Ref. [15], the strong coupling limit provides a complementary view to the shell model calculations which become more challenging for heavier nuclei. Applications to other Islands of Inversions will be the subject of a future publication.

Acknowledgments

Enlightening discussions with Profs. R. F. Casten, R. Kanungo, and J. P. Schiffer are gratefully acknowledged. This material is based upon work supported by the U.S. Department of Energy, Office of Science, Office of Nuclear Physics under Contract No. DE-AC02-05CH11231 (LBNL) and Grant No. DE-FG02-88ER40387 (OU).

[1] Kris Heyde and John L. Wood, Reviews of Modern Physics, Vol. 83, 1467 (2011).
[2] K. Heyde and J. L. Wood, Phys. Scr. 91 083008 (2016).
[3] O. Sorlin and M. Porquet, Prog. Part. Nucl. Phys. **61**, 602 (2008).
[4] T. Otsuka *et al.*, Phys. Rev. Lett **87**, 082502 (2001).
[5] X. Campi, H. Flocard, A. K. Kerman and S. Koonin, Nucl. Phys. A 251, 193 (1975).
[6] A. Poves and J. Retamosa, Phys. Lett. **B184**, 311 (1987).
[7] C. Thibault *et al.*, Phys. Rev. C **12**, 644 (1975).
[8] E. K. Warburton, J. A. Becker and B. A. Brown, Phys. Rev. C **41**, 1147 (1990).
[9] P.G. Hansen and J.A. Tostevin, Ann. Rev. of Nuclear and Particle Science, Vol 53, 219 (2003).
[10] A.P. Zuker, *et al.* Phys. Rev. C **92**, 024320 (2015).
[11] S. G. Nilsson and I. Ragnarsson, Shapes and Shells in Nuclear Structure, Cambridge University Press, 1995.
[12] H. Mach *et al.*, Eur. Phys. J. A **25** 105 (2005).
[13] G. Neyens, *et al.*, Phys. Rev. Lett. **94**, 022501 (2005).
[14] P. Himpe *et al.*, Phys. Lett. **643** 257 (2006).
[15] A. Richard, *et al.*, Phys. Rev. **C96**, 011303(R), (2017).
[16] D. .T. Yordanov, *et al.*, Phys. Rev. Lett. **99**, 212501 (2007).
[17] I. Hamamoto, Phys. Rev. C **76**, 054319 (2007).
[18] B. Elbek and P. Tjom, Advances in Nucl. Phys. Vol 3, **259** (1969).
[19] A. J. Howard *et al.*, Nuclear Physics A **150** (1970) 609.
[20] J. Janecke, Nuclear Physics A **204** (1973) 497.
[21] R. Kanungo, et al., Phys. Lett. B685, 253 (2010).
[22] U. Datta et al. Phys. Rev. C **94**, 034304(R) (2016).
[23] B .E. Chi, Nuclear Physics A **83** 97 (1966).
[24] S. E. Larsson, G. Leander and I. Ragnarsson, Nuclear Physics A307 (1978) 189.
[25] H. L. Crawford *et al.*, Phys. Rev. C **93**, 031303(R) (2016).
[26] J. R. Terry *et al.*, Phys. Rev. C 77, 014316 (2008)